Kotobuki N, Hirose M, Machida H, Katou Y, Muraki K, Takakura Y, Ohgushi H	Viability and Osteogenic Potential of Cryopreserved Human Bone Marrow-Derived Mesenchymal Cells	Tissue Engineering	11	663-673	2005
竹下　聡	血管新生療法	治療学	39	775-777	2005
Sekiya S, Shimizu T, Yamato M, Kikuchi A, Okano T,	Bioengineered cardiac cell sheet grafts have intrinsic angiogenic potential	Biochemical and Biophysical Research Communications	341	573-582	2006
Shimizu T, Sekine H, Yang J, Isoi Y, Yamato M, Kikuchi A, Kobayashi E, Okano T,	Polysurgery of cell sheet grafts overcomes diffusion limits to produce thick, vascularized myocardial tissues	The FASEB Journal			2006 In press
清水達也、 岡野光夫	Ⅱ.心筋の再生・心筋再生の現状と今後の展望	再生医療	4(3)	383-390	2005
清水達也	心筋再生　2) 組織工学による心筋再生	ICU と CCU	29(7)	539-546	2005
Hattan, N., Kawaguchi, H., Ando, K., Kuwabara, E., Fujita, J., Murata, M., Suematsu, M., Mori, H., Fukuda K	Purified cardiomyocytes from bone marrow mesenchymal stem cells produce stable intracardiac grafts in mice.	Cardiovasc. Res.	65	334-344	2005
Fujii, T., Nagaya, N., Iwase, T., Murakami, S., Miyahara, Y., Nishigami, K., Ishibashi-Ueda, H., Shirai, M., Itoh, T., Ishino, K., Sano, S., Kangawa, K., Mori, H.	Adrenomedullin enhances therapeutic potency of bone marrow transplantation for myocardial infarction in rats.	Am. J. Physiol. Heart. Circ. Physiol.	288	H1444 - H1450	2005

Kitagawa, H., Yamazaki, T., Akiyama, T., Sugimachi, M., Sunagawa, K., Mori, H.	Microdialysis separately monitors myocardial interstitial myoglobin during ischemic and reperfusion.	Am.J.Physiol.Heart.Circ.Physiol.	289	H924-H930	2005
Kuroko, Y., Fujii, T., Yamazaki, T., Akiyama, T., Ishino, K., Sano, S., Mori H.	Contribution of catechol O-methyltransferase to the removal of accumulated interstitial catecholamines evoked by myocardial ischemia.	Neuroscience Letters	388	61-64	2005
中谷武嗣、永谷憲歳、富田伸司	心筋再生	綜合臨牀	54	91-97	2005
中谷武嗣	治療の進歩　補助人工心臓	日本内科学会雑誌	94	111-118	2005
中谷武嗣、 花谷彰久	補助人工心臓	ICU と CCU	29	265-273	2005
中谷武嗣	日本における心臓移植の現況	今日の移植	18	287-293	2005
中谷武嗣、富田伸司、永谷憲歳	重症心不全に対する幹細胞による心筋再生療法の開発	再生医療	4	399-403	2005
中谷武嗣、高野久輝	心臓補助循環の実際	呼吸と循環	53	1289-1295	2005
菅　理晴、藤里俊哉、永谷憲歳、中谷武嗣	ブタ組織の脱細胞化	日本移植学会雑誌	40	441-444	2005
Fukuhara S, Tomita S, Tomita S, Nakatani T, Yutani C, Kitamura S.	Endogenous bone-marrow-derived stem cells contribute only a small proportion of regenerated myocardium in the acute infarction model.	J. Heart and Lung Transplant	24	67-72	2005

Asaumi Y, Yasuda S, Morii I, Kakuchi H, Otsuka Y, Kawamura A, Sasako Y, Nakatani T, Nonogi H and Miyazaki S.	Favourable clinical outcome in patients with cardiogenic shock due to fulminant myocarditis supported by percutaneous extracorporeal membrane oxygenation.	European Heart Journal	26	2185-2192	2005
Omoto R, Kyo S, Nishimura M, Matsuda H, Matsumiya G, Kitamura S, Nakatani T, Takamoto S, Ono M, Tabayashi K, Yozu R.	Japanese multicenter clinical evaluation of the HeartMate vented electric left ventricular assist system.	J Artif Organs	8	34-40	2005
Kosuge M, Kimura K, Kojima S, Sakamoto T, Ishihara M, Asada Y, Tei C, Miyazaki S, Sonoda M, Tsuchihashi K, Yamagishi M, Ikeda Y, Shirai M, Hiraoka H, Inoue T, Saito F, Ogawa H	on behalf of the Japanese Acute Coronary Syndrome Study (JACSS) Investigators.	Circ J.	70(3)	217-21	2006
Maruo T, Nakatani S, Kanzaki H, Kakuchi H, Yamagishi M, Kitakaze M, Ohe T, Miyatake K.	Circadian variation of endothelial function in idiopathic dilated cardiomyopathy.	Am J Cardiol.	97(5)	699-702	2006

Kojima S, Sakamoto T, Ishihara M, Kimura K, Miyazaki S, Yamagishi M, Tei C, Hiraoka H, Sonoda M, Tsuchihashi K, Shimoyama N, Honda T, Ogata Y, Matsui K, Ogawa H	Japanese Acute Coronary Syndrome Study (JACSS) Investigators. Prognostic usefulness of serum uric acid after acute myocardial infarction (the Japanese Acute Coronary Syndrome Study).	Am J Cardiol	96(4)	489-95	2005
Kosuge M, Kimura K, Kojima S, Sakamoto T, Ishihara M, Asada Y, Tei C, Miyazaki S, Sonoda M, Tsuchihashi K, Yamagishi M, Ikeda Y, Shirai M, Hiraoka H, Inoue T, Saito F, Ogawa H	Japanese Acute Coronary Syndrome Study (JACSS) Investigators. Beneficial effect of preinfarction angina on in-hospital outcome is preserved in elderly patients undergoing coronary intervention for anterior acute myocardial infarction.	Circ J.	69(6)	630-5	2005
Kosuge M, Kimura K, Kojima S, Sakamoto T, Matsui K, Ishihara M, Asada Y, Tei C, Miyazaki S, Sonoda M, Tsuchihashi K, Yamagishi M, Ikeda Y, Shirai M, Hiraoka H, Inoue T, Saito F, Ogawa H	Japanese Acute Coronary Syndrome Study (JACSS) Investigators. Effects of glucose abnormalities on in-hospital outcome after coronary intervention for acute myocardial infarction.	Circ J	69(4)	375-9	2005
Ogata T, Yasaka M, Yamagishi M, Seguchi O, Nagatsuka K, Minematsu K.	Atherosclerosis found on carotid ultrasonography is associated with atherosclerosis on coronary intravascular ultrasonography.	J Ultrasound Med.	24(4)	469-74	2005

Lazarevic AM, Nakatani S, Okita Y, Marinkovic J, Takeda Y, Hirooka K, Matsuo H, Kitamura S, Yamagishi M, Miyatake K.	Determinants of rapid progression of aortic root dilatation and complications in Marfan syndrome.	Int J Cardiol.	106(2)	177-82	2006
Ishihara M, Kojima S, Sakamoto T, Asada Y, Tei C, Kimura K, Miyazaki S, Sonoda M, Tsuchihashi K, Yamagishi M, Ikeda Y, Shirai M, Hiraoka H, Inoue T, Saito F, Ogawa H	Japanese Acute Coronary Syndrome Study Investigators. Acute hyperglycemia is associated with adverse outcome after acute myocardial infarction in the coronary intervention era.	Am Heart J.	150(4)	814-20	2005
Saito S, Kobayashi J, Tagusari O, Bando K, Niwaya K, Nakajima H, Yamagishi M, Yagihara T, Kitamura S.	Successful excision of a cystic tumor of the atrioventricular nodal region.	Circ J.	69(10)	1293-4	2005
Higo S, Uematsu M, Yamagishi M, Ishibashi-Ueda H, Awata M, Morozumi T, Ohara T, Nanto S, Nagata S.	Elevation of plasma matrix metalloproteinase-9 in the culprit coronary artery in patients with acute myocardial infarction: clinical evidence from distal protection.	Circ J.	69(10)	1180-5	2005

Shimizu W, Aiba T, Antzelevitch C	Specific therapy based on the genotype and cellular mechanism in inherited cardiac arrhythmias. - Long QT syndrome and Brugada syndrome -.	Curr Pharm Design	11	1561-1572	2005
Shimizu W	The long QT syndrome: Therapeutic implications of a genetic diagnosis.	Cardiovasc Res	67	347-356	2005
Shimizu W, Aiba T, Kamakura S	Mechanisms of disease: current understanding and future challenges in Brugada syndrome.	Nat Clin Pract Cardiovasc Med	2	408-414	2005
Shimizu W	Acquired Forms of the Brugada Syndrome.	J Electrocardiol	38	22-25	2005
Shimizu W	The Brugada Syndrome. - An update -.	Internal Med	44	1224-1231	2005
Antzelevitch C, Brugada P, Borggrefe M, Brugada J, Brugada R, Corrado D, Gussak I, Lemarec H, Nademanee K, Perez Riera AR, Shimizu W,	Schulze-Bahr E, Tan H, Wilde A: Brugada Syndrome. Report of the Second Consensus Conference. Endorsed by the Heart Rhythm Society and the European Heart Rhythm Association.	Circulation	111	659-670	2005

Aiba T, Shimizu W, Inagaki M, Noda T, Miyoshi S, Ding WG, Zankov DP, Toyoda F, Matsuura H, Horie M, Sunagawa K	Cellular and ionic mechanism for drug-induced long-QT syndrome and effectiveness of verapamil.	J Am Coll Cardiol	45	300-307	2005
Maekawa K, Saito Y, Ozawa S, Adachi-Akahane S, Kawamoto M, Komamura K, Shimizu W, Ueno K, Kamakura S, Kamatani N, Kitakaze M, Sawad J	Genetic polymorphisms and haplotypes of the human cardiac sodium channel α subunit gene (SCN5A) in Japanese and their association with arrhythmia.	Ann Hum Genet	69	413-428	2005
Satomi K, Shimizu W, Takaki H, Suyama K, Kurita T, Aihara N, Kamakura S	Response of beat-by-beat QT variability to sympathetic stimulation in LQT1 form of congenital long QT syndrome.	Heart Rhythm	2	149-154	2005
Noda T, Shimizu W, Taguchi A, Aiba T, Satomi K, Suyama K, Kurita T, Aihara N, Kamakura S	Malignant entity of idiopathic ventricular fibrillation and polymorphic ventricular tachycardia initiated by premature extrasystoles originating from right ventricular outflow tract.	J Am Coll Cardiol	46	1288-1294	2005
Noda T, Shimizu W, Suyama K, Tobiume T, Satomi K, Kurita T, Aihara N, Kamakura S:	Permanent Form of Junctional Reciprocating Tachycardia Accompanied by Atrial Tachycardia.	Circ J	69	1003-1006	2005

Satomi K, Shimizu W	Implications and problems of sudden cardiac death in the heart failure trial (SCD-Heft).	Future Cardiology	1	599-603	2005
Shimizu W	Editorial comment. Does an overlap syndrome really exist between Brugada syndrome and progressive cardiac conduction defect (Lenegre syndrome)?	J Cardiovasc Electrophysiol	17		2006 in press
Bezzina CR*, Shimizu W*, Yang P*, Koopmann TT, Tanck MWT, Miyamoto Y, Kamakura S, Roden DM, Wilde AAM	A common sodium channel promoter haplotype in Asian subjects underlies variability in cardiac conduction.	Circulation	113	338-344	2006 * These 3 authours equally contributed
Kandori A, Miyashita T, Ogata K, Shimizu W, Yokokawa M, Kamakura S, Miyatake K, Tsukada K, Yamada S, Watanabe S, Yamaguchi I	Electrical space-time abnormalities of ventricular depolarization in patients with brugada syndrome and patients with complete right-bundle branch blocks studied by magnetocardiography.	PACE	29	15-20	2006
Aiba T, Shimizu W, Hidaka I, Uemura K, Noda T, Zheng C, Kamiya A, Inagaki M, Sugimachi M, Sunagawa K	Cellular basis for trigger and maintenance of ventricular fibrillation in the Brugada syndrome model: High resolution optical mapping study.	J Am Coll Cardiol			2006 in press

Ogata K, Kandori A, Miyashita T, Tsukada K, Nakatani S, Shimizu W, Kanzaki H, Miyatake K, Yamada S, Yamada S, Watanabe S, Yamaguchi I	Visualization of three-dimensional cardiac electrical excitation using standard heart model and anterior and posterior magnetocardiogram.	Int J Cardiovas Imag			2006 in press
Nagai T, Suyama K, Shimizu W, Noda T, Satomi K, Kurita T, Aihara N, Kamakura S	Pilsicainide-induced verapamil sensitive idiopathic left ventricular tachycardia.	PACE			2006 in press
Kitamura S, Satomi K, Kurita T, Shimizu W, Suyama K, Aihara N, Niwaya K, Kobayashi J, Kamakura S	Long term follow-up of transvenous defibrillation leads: High incidence of lead fracture.	Circ J			2006 in press
Otomo K, Okamura H, Noda T, Satomi K, Shimizu W, Suyama K, Kurita T, Aihara N, Kamakura S	Unique electrophysiological characteristics of atrioventricular nodal reentrant tachycardia with different ventriculo-atrial block patterns: Effects of slow pathway ablation and insights into location of reentrant circuit.	Heart Rhythm			2006 in press
Shimizu W, Antzelevitch C	Long QT syndrome. in Lang F (ed): Molecular mechanisms of disease	an Encyclopedic reference, Springer, UK,			2006 in press

nature medicine

Monolayered mesenchymal stem cells repair scarred myocardium after myocardial infarction

Yoshinori Miyahara[1,9], Noritoshi Nagaya[1,9], Masaharu Kataoka[1], Bobby Yanagawa[1], Koichi Tanaka[1], Hiroyuki Hao[2], Kozo Ishino[3], Hideyuki Ishida[4], Tatsuya Shimizu[5], Kenji Kangawa[6], Shunji Sano[3], Teruo Okano[5], Soichiro Kitamura[7] & Hidezo Mori[8]

Mesenchymal stem cells are multipotent cells that can differentiate into cardiomyocytes and vascular endothelial cells. Here we show, using cell sheet technology, that monolayered mesenchymal stem cells have multipotent and self-propagating properties after transplantation into infarcted rat hearts. We cultured adipose tissue–derived mesenchymal stem cells characterized by flow cytometry using temperature-responsive culture dishes. Four weeks after coronary ligation, we transplanted the monolayered mesenchymal stem cells onto the scarred myocardium. After transplantation, the engrafted sheet gradually grew to form a thick stratum that included newly formed vessels, undifferentiated cells and few cardiomyocytes. The mesenchymal stem cell sheet also acted through paracrine pathways to trigger angiogenesis. Unlike a fibroblast cell sheet, the monolayered mesenchymal stem cells reversed wall thinning in the scar area and improved cardiac function in rats with myocardial infarction. Thus, transplantation of monolayered mesenchymal stem cells may be a new therapeutic strategy for cardiac tissue regeneration.

Myocardial infarction, a main cause of heart failure, leads to loss of cardiac tissue and impairment of left ventricular function. Therefore, restoring the scarred myocardium is desirable for the treatment of heart failure. Although needle injections of bone marrow cells into the myocardium have been performed for cardiac regeneration[1–5], it is difficult to reconstruct sufficient cardiac mass in the thinned scar area after myocardial infarction.

Recently, our colleagues have developed cell sheets using temperature-responsive culture dishes[6]. These cell sheets allow for cell-to-cell connections and maintain the presence of adhesion proteins because enzymatic digestion is not needed[7–10]. Therefore, cell sheet transplantation may be a promising strategy for partial cardiac tissue reconstruction. Skeletal myoblasts, fetal cardiomyocytes and embryonic stem cells have been considered as candidates for an implantable cell source[11–13]. It is difficult, however, to produce a multilayered construct requiring a vascular network. Thus, autologous somatic stem cells with self-propagating properties that can induce angiogenesis are a desirable cell source for a transplantable sheet.

Mesenchymal stem cells (MSCs) are multipotent adult stem cells that reside within the bone marrow microenvironment[14,15]. MSCs can differentiate not only into osteoblasts, chondrocytes, neurons and skeletal muscle cells, but also into vascular endothelial cells[16] and cardiomyocytes[17–20]. In contrast to their hematopoietic counterparts, MSCs are adherent and can expand in culture. Recently, MSCs have been isolated from adipose tissue[21–24], which is typically abundant in individuals with cardiovascular disease. Here, we investigated the therapeutic potency of monolayered MSCs derived from adipose tissue using cell sheet technology.

RESULTS

Characteristics of adipose tissue–derived MSCs

We isolated MSCs from subcutaneous adipose tissue of male Sprague-Dawley rats on the basis of the adherent properties of these cells. We obtained $1.7 \times 10^5 \pm 0.2 \times 10^5$ cells from 1 g adipose tissue in a 12-h culture. By day 4 of culture of the minced adipose tissue, spindle-shaped adherent cells were apparent and formed symmetric colonies. After approximately three to four passages, most adherent cells expressed CD29 and CD90 (**Supplementary Fig. 1** online). In contrast, the majority of adherent cells were negative for CD34 and CD45. They were also negative for CD31, a marker for vascular endothelial cells, and negative for α smooth muscle actin (αSMA), a marker for smooth muscle cells. A small fraction of adherent cells expressed CD71, CD106 and CD117. These results were similar to those from bone marrow–derived MSCs[15,22,25] (**Supplementary Fig. 1** online). Using previously described methods[16,22,26], we confirmed that these adipose-derived adherent cells, like bone marrow–derived MSCs, were multipotent, as judged by their ability to differentiate into adipocytes, osteoblasts and vascular endothelial cells. Thus, we

[1]Department of Regenerative Medicine and Tissue Engineering, National Cardiovascular Center Research Institute and [2]Department of Pathology, National Cardiovascular Center, 5-7-1 Fujishirodai, Suita, Osaka, 565-8565, Japan. [3]Department of Cardiovascular Surgery, Okayama University Graduate School of Medicine, Dentistry and Pharmaceutical Sciences, 2-5-1 Shikata-cho, Okayama, 700-8555, Japan. [4]Department of Physiology, School of Medicine, Tokai University, Bohseidai, Isehara, Kanagawa, 259-1193, Japan. [5]Institute of Advanced Biomedical Engineering and Science, Tokyo Woman's Medical University, 8-1 Kawada-cho, Shinjuku-ku, Tokyo, 162-8666, Japan. [6]Department of Biochemistry, National Cardiovascular Center Research Institute and [7]Department of Cardiovascular Surgery, National Cardiovascular Center and [8]Department of Cardiac Physiology, National Cardiovascular Center Research Institute, 5-7-1 Fujishirodai, Suita, Osaka, 565-8565, Japan. [9]These authors contributed equally to this work. Correspondence should be addressed to N.N. (nnagaya@ri.ncvc.go.jp) or H.M. (hidemori@ri.ncvc.go.jp).

Received 9 August 2005; accepted 3 March 2006; published online XX XX 2006; doi:10.1038/nmXXXX

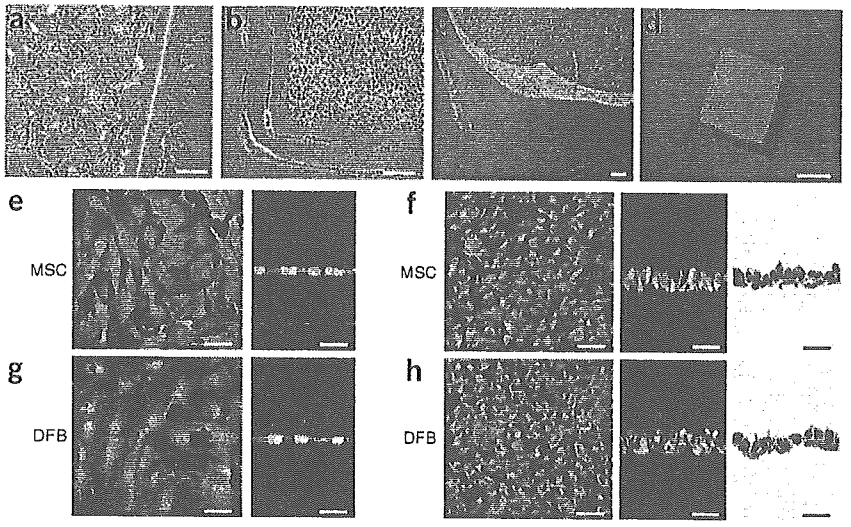

Figure 1 Preparation of monolayered MSCs. (**a**) MSCs 2 d after seeding on a temperature-responsive dish. (**b**) Cultured MSCs expanded to confluence within the square area of the dish by day 3. (**c**) The monolayered MSCs detached easily from the culture dish at 20 °C. (**d**) The completely detached monolayered MSCs were identified as a 12 × 12 mm square sheet. (**e–h**) Cross-sectional analysis of GFP-expressing monolayered MSCs and DFBs before detachment (**e** and **g**, confocal images) and after detachment (**f** and **h**, left and center, confocal images; right, Masson trichrome). The thickness of both monolayers was 3.5-fold greater than the thickness before detachment, and constituent cells were compacted. Scale bars in **a–c**, 100 μm; in **d**, 5 mm; in **e–h**, 20 μm.

confirmed that the majority of adherent cells isolated from adipose tissue were MSCs.

Preparation and transplantation of monolayered MSCs

We cultured adipose tissue–derived MSCs (5×10^5 cells) on temperature-responsive dishes for 3 d until confluent. MSCs were attached on the poly-*N*-isopropylacrylamide (PIPAAm)-grafted area (24 × 24 mm; **Fig. 1a,b**). As the culture temperature was decreased from 37 °C to 20 °C, MSCs detached spontaneously and floated up into the culture medium as a monolayer of MSCs within 40 min (**Fig. 1c,d**). As a control, we prepared dermal fibroblasts (DFBs) by the skin explant technique[27]. DFBs (8×10^5 cells) were cultured on the temperature-responsive dishes, and monolayered DFBs were fabricated as described above. The final cell counts for monolayered MSCs and DFBs before transplantation were $9.4 \pm 0.6 \times 10^5$ and $8.6 \pm 0.6 \times 10^5$ cells, respectively ($n = 6$ each). To identify the thickness of monolayered MSCs, we used green fluorescent protein (GFP)-expressing cell grafts derived from the GFP-transgenic Sprague-Dawley rats. Immediately after detachment, cells became compacted, possibly owing to cytoskeletal tensile reorganization, and the thickness of monolayered MSCs and DFBs was approximately 3.5-fold greater than the thickness before detachment (MSCs, 6.2 ± 0.3 to 21.5 ± 0.8 μm; DFBs, 6.5 ± 0.4 to 22.4 ± 1.1 μm; **Fig. 1e–h**). MSCs on the temperature-responsive dishes were positive for vimentin and slightly positive for collagen type 1, whereas DFBs were positive for both markers (**Fig. 2a**). We transferred detached monolayered MSCs above the myocardial scar (**Fig. 2b**) and then attached them to the surface of the anterior scar (**Fig. 2c**).

Secretion of angiogenic factors from monolayered MSCs

We measured secretion of angiogenic factors from MSCs 24 h after monolayers had formed, equivalent to day 4 after initial cell seeding. The monolayered MSCs secreted significantly larger amounts of angiogenic and antiapoptotic factors such as vascular endothelial growth factor (VEGF) and hepatocyte growth factor (HGF) than did the monolayered DFBs ($P < 0.01$; **Fig. 2d**). The control medium supplemented with 10% fetal calf serum contained less than 5 pg/ml of VEGF or HGF. These results suggest that the paracrine effects of monolayered MSCs on host myocardium are greater than those of monolayered DFBs.

Engraftment and growth of monolayered MSCs

To identify the transplanted cells in myocardial sections, we used GFP-expressing cell grafts derived from the GFP-transgenic Sprague-Dawley rats. We grafted monolayered MSCs or DFBs onto the scar area of the anterior wall (**Fig. 3**). Fluorescence microscopy showed that GFP-expressing monolayered MSCs gradually grew *in situ* and developed into a thick stratum, up to ~600 μm thick over the native tissue at 4 weeks (**Fig. 3a–f**). The engrafted MSC tissue tapered off toward the healthy myocardium (**Fig. 3d,e**), although most of the monolayered MSCs were attached only to the scar area in the anterior wall because of the large infarct. We rarely detected TUNEL-positive MSCs in the sheet (<1%) 48 h after transplantation (**Fig. 3g**), implying that cell viability in the sheet was maintained. In contrast, we frequently detected TUNEL-positive cells (15% ± 2%) in the DFB sheet, which was observed as a thin layer above the scar. Subsequently, the DFB sheet was undetectable 1 week later. Masson trichrome staining showed increased thickness of the anterior wall and attenuation of left ventricle enlargement after transplantation of monolayered MSCs (**Fig. 3h**), although the infarct size did not differ significantly among the untreated, DFB and MSC groups (**Supplementary Table 1** online).

Reconstruction of cardiac mass

After growth *in situ*, GFP-expressing MSC tissue contained a number of mature vascular structures that had positive staining for von Willebrand factor (vWF) and αSMA (**Fig. 4a,b**). A small fraction of the MSC tissue had positive staining for cardiac troponin T and desmin (**Fig. 4c,d**). On the other hand, a large proportion of the MSC tissue was positive for vimentin, a marker for mesenchymal lineage cells (**Fig. 4e**). The percentages of graft-derived cells that expressed endothelial (vWF), smooth muscle (αSMA), cardiac (troponin T) and mesenchymal (vimentin) markers were 12.2% ± 0.6%, 5.0% ± 0.3%, 5.3% ± 0.3% and 57.8% ± 2.2%, respectively. Notably, based on expression of these markers, two-thirds of vascular endothelial cells, four-fifths of smooth muscle cells and one-twentieth of cardiomyocytes within the MSC tissue were GFP^- and hence were derived from the host. The MSC tissue stained modestly for collagen type 1 (**Fig. 4f**). Picrosirius red staining showed that collagen deposition was found mainly in the extracellular matrix and the epicardial margin of the MSC tissue (**Fig. 4g**). Excluding staining in blood vessels, the MSC tissue was also negative for αSMA, a marker for myofibroblasts (**Fig. 4b**). This phenotype was consistent with properties of MSCs

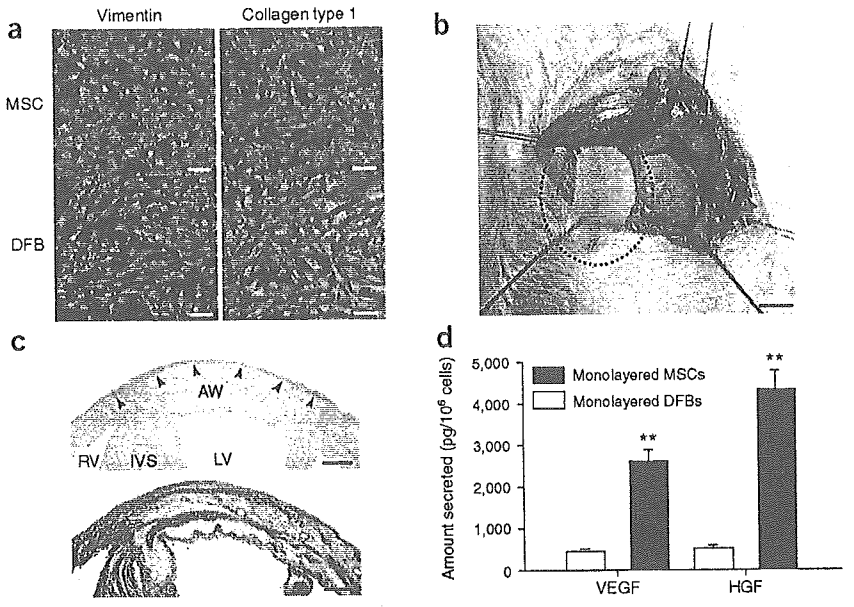

Figure 2 Characteristics of monolayered MSCs. (**a**) Properties of constituent cells in the monolayered grafts. Compared with DFBs (green), MSCs (green) are positive for vimentin (red) and slightly positive for collagen type 1 (red). (**b**) Monolayered MSCs (in the dotted circle) transferred to the infarcted heart. (**c**) Extent of monolayered MSCs 48 h after transplantation (arrows). AW, anterior wall; LV, left ventricle; RV right ventricle; IVS, interventricular septum. (**d**) Comparison of secretion of growth factors between monolayered MSCs and DFBs. Scale bar in **a**, 20 μm; in **b**, 5 mm; in **c**, 100 μm.

before transplantation (**Fig. 2a** and **Supplementary Fig. 1** online), suggesting that the MSC tissue includes a number of undifferentiated MSCs. Taken together, the grown MSC tissue was composed of newly formed blood vessels, undifferentiated MSCs and few cardiomyocytes.

Fluorescence *in situ* hybridization analysis

We performed fluorescence *in situ* hybridization (FISH) to detect X and Y chromosomes after sex-mismatched transplantation of monolayered MSCs. We transplanted GFP-expressing monolayered MSCs derived from male rats to female Sprague-Dawley rats that had suffered an infarct. Four weeks later, newly formed cardiomyocytes that were positive for GFP had only one set of X and Y chromosomes, whereas we detected two X chromosomes exclusively in GFP^- host-derived cells (**Fig. 4h**). We counted the X and Y chromosomes in male and female control rats and in the MSC sheet–transplanted rats (**Supplementary Table 2** online), and we did not detect extra copies of the X or Y chromosome in graft-derived GFP^+ cardiomyocytes. When we compared the frequencies of the occurrence of zero, one, two and more than two X chromosomes in the GFP^+ cardiomyocytes with the frequencies in male control cardiomyocytes, the GFP^+ cardiomyocytes did not show an increased proportion of X chromosomes ($0.25 > P > 0.10$, χ^2 test).

Effects of monolayered MSCs on cardiac function

Heart failure developed 8 weeks after coronary ligation, as indicated by an increase in left ventricle end-diastolic pressure (LVEDP) and attenuation of left ventricle maximum and minimum rate of increase of left ventricular pressure (dP/dt). Autologous transplantation of monolayered MSCs, however, resulted in decreased LVEDP (**Fig. 5a**). Left ventricle maximum and minimum dP/dt were significantly improved in the MSC group (**Fig. 5b,c**). We did not observe these hemodynamic improvements in the DFB group. The MSC group also had significantly lower right ventricular weight and lung weight than the DFB and untreated groups 4 weeks after transplantation (**Supplementary Table 1** online). These results suggest that transplantation of monolayered MSCs has beneficial hemodynamic effects in rats with chronic heart failure.

Echocardiographic analysis showed that transplantation of monolayered MSCs significantly increased diastolic thickness of the infarcted anterior wall (**Fig. 5d**). Left ventricle end-diastolic dimension at 8 weeks was significantly smaller in the MSC group than in the DFB and untreated groups (**Fig. 5e**). Transplantation of the monolayered MSCs significantly increased left ventricle fractional shortening (**Fig. 5f**). Left ventricle wall stress in diastole was markedly lower in the MSC group than in the DFB and untreated groups (**Supplementary Table 3** online). Plasma atrial natriuretic peptide (ANP) in the DFB and untreated groups was markedly elevated 8 weeks after myocardial infarction (**Fig. 5g**). Transplantation of the monolayered MSCs inhibited the increase in plasma ANP.

Survival analysis

The Kaplan-Meier survival curve showed that 4-week survival after coronary ligation did not differ significantly between the untreated and MSC groups before transplantation (**Fig. 5h**). Notably, however, no rats died after transplantation of monolayered MSCs. Therefore, the survival rate after transplantation was markedly higher in the MSC group than in the untreated group (4-week survival after transplantation was 100% for the MSC group versus 71% for the untreated group, log-rank test, $P < 0.05$).

DISCUSSION

There are several advantages to monolayered MSC transplantation. First, the self-propagating property of MSCs *in situ* leads to the formation of a thick stratum on the surface of the scarred myocardium. Second, the multipotency of MSCs and their ability to supply angiogenic cytokines allows neovascularization in the MSC tissue. Third, the reconstruction of thick myocardial tissue reduces left ventricle wall stress and results in improvement of cardiac function after myocardial infarction. Finally, a substantial part of the transplanted tissue is composed of undifferentiated MSCs, and it is tempting to speculate that such cells may act against future progressive left ventricle remodeling.

Cellular cardiomyoplasty using needle injections is emerging as a treatment option for individuals with chronic heart failure, but it may be limited by failure to regenerate cardiac mass. The cell sheet allows for cell-to-cell connections owing to the lack a need for enzymatic digestion[6–10]. Thus, the cell sheet has attracted considerable interest as a tool for tissue engineering[28]. Here, we used adipose tissue–derived MSCs as a cellular source for the cell sheet, which resulted in successful autologous transplantation in heterogenic rats without immunological rejection. Using flow cytometry, we did not find any substantial

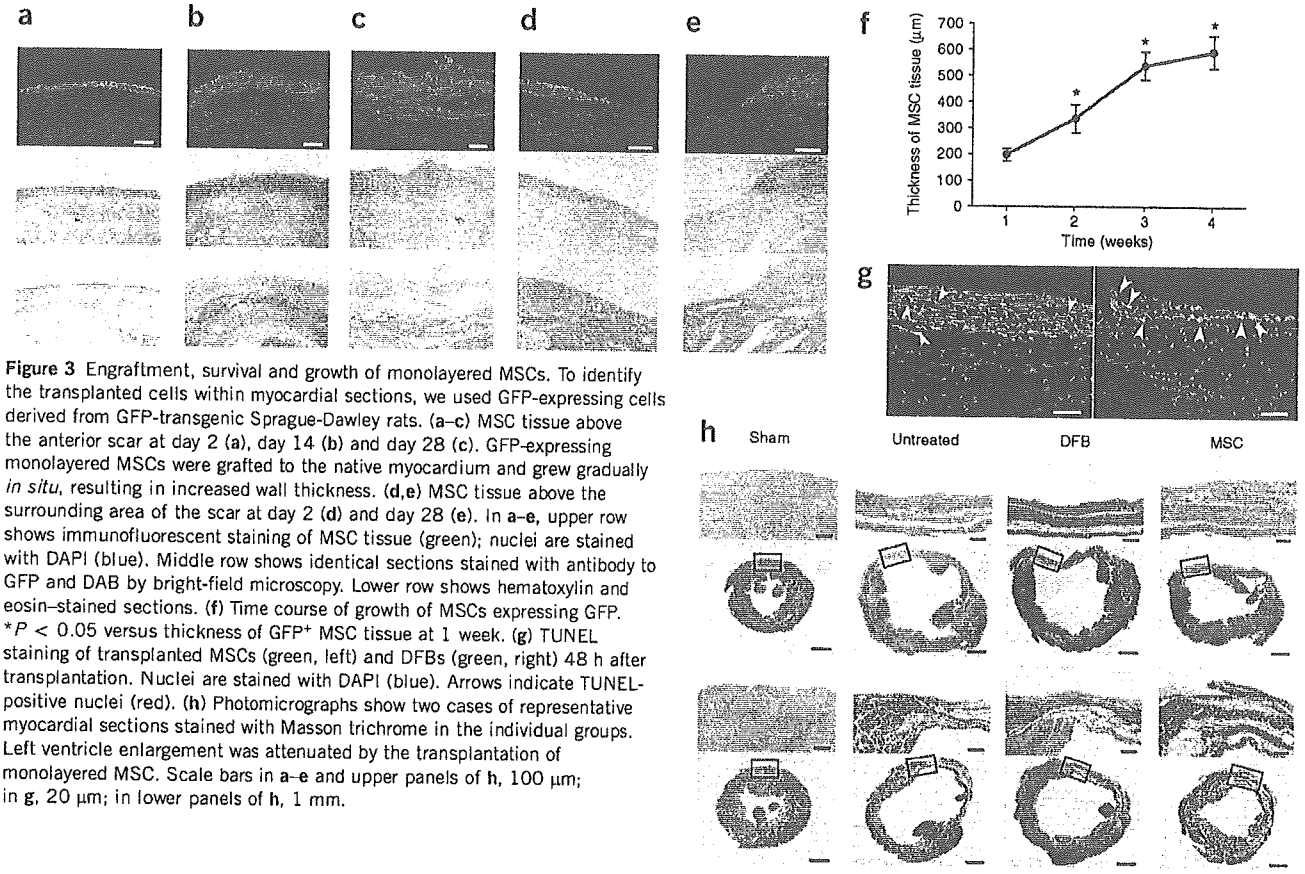

Figure 3 Engraftment, survival and growth of monolayered MSCs. To identify the transplanted cells within myocardial sections, we used GFP-expressing cells derived from GFP-transgenic Sprague-Dawley rats. (**a–c**) MSC tissue above the anterior scar at day 2 (**a**), day 14 (**b**) and day 28 (**c**). GFP-expressing monolayered MSCs were grafted to the native myocardium and grew gradually *in situ*, resulting in increased wall thickness. (**d,e**) MSC tissue above the surrounding area of the scar at day 2 (**d**) and day 28 (**e**). In **a–e**, upper row shows immunofluorescent staining of MSC tissue (green); nuclei are stained with DAPI (blue). Middle row shows identical sections stained with antibody to GFP and DAB by bright-field microscopy. Lower row shows hematoxylin and eosin–stained sections. (**f**) Time course of growth of MSCs expressing GFP. $^*P < 0.05$ versus thickness of GFP$^+$ MSC tissue at 1 week. (**g**) TUNEL staining of transplanted MSCs (green, left) and DFBs (green, right) 48 h after transplantation. Nuclei are stained with DAPI (blue). Arrows indicate TUNEL-positive nuclei (red). (**h**) Photomicrographs show two cases of representative myocardial sections stained with Masson trichrome in the individual groups. Left ventricle enlargement was attenuated by the transplantation of monolayered MSC. Scale bars in **a–e** and upper panels of **h**, 100 μm; in **g**, 20 μm; in lower panels of **h**, 1 mm.

differences between adipose tissue–derived MSCs and bone marrow–derived MSCs, consistent with results from previous studies[22,25]. Adipose-derived MSCs readily attached to and propagated on the temperature-responsive dish. Abdominal subcutaneous adipose tissue is clinically redundant and easily accessible by rapid and minimally invasive surgery such as liposuction. Thus, adipose tissue may serve as a source of stem cells for therapeutic cell sheets.

Here, monolayered MSCs could readily be transferred and grafted to the scarred myocardium without additives or suturing. This may be attributable to cell-to-cell connections as well as extracellular matrix deposits on the basal surface of the monolayered MSCs. Regeneration of myocardial mass is thought to require multilayered constructs of the cell sheet. Unfortunately, however, the lack of a vascular network has limited the formation of a thick construct[10,29]. The transplanted monolayered MSCs thickened gradually, developing into a stratum of up to 600 μm in thickness over the native tissue 4 weeks after transplantation, suggesting that monolayered MSCs have an ability to grow *in situ*. As a result, the transplanted MSC tissue reversed wall thinning of the infarcted myocardium. On the other hand, the fibroblast sheet did not grow *in situ*. It should be noted that the MSC tissue included a large number of newly formed blood vessels. These vessels were composed of graft-derived cells, host-derived cells or both. The MSC sheet secreted a large amount of angiogenic and antiapoptotic cytokines, including VEGF and HGF, as compared with the fibroblast sheet. These results suggest that MSCs induce neovascularization within the sheet not only through their ability to differentiate into vascular cells but also through growth factor–mediated paracrine regulation. Thus, we believe that the angiogenic action of MSCs is important for reconstruction of cardiac mass by the MSC tissue.

Four weeks after transplantation, a small fraction of the engrafted MSCs were positive for cardiac proteins such as cardiac troponin T and desmin, suggesting the presence of cardiomyocytes within the MSC tissue. FISH analysis suggested that the most cardiomyocytes within the MSC tissue were not derived from cell fusion, but we are unable to exclude the possibility that some were. Further studies are necessary to investigate the mechanisms by which MSCs within the MSC tissue regenerate cardiomyocytes. The majority of the MSC tissue was positive for vimentin, a marker for undifferentiated MSCs and fibroblasts. In addition, the majority of MSCs within the graft were negative for collagen type 1 and αSMA, a marker for myofibroblasts. These results suggest that the grown-up MSC tissue is composed of newly formed blood vessels, undifferentiated MSCs and few cardiomyocytes.

We have also shown that transplantation of the monolayered MSCs significantly increased left ventricle maximum dP/dt, decreased LVEDP and inhibited the development of left ventricle enlargement in rats with chronic heart failure secondary to myocardial infarction. These results suggest that transplantation of monolayered MSCs improves cardiac function. But the presence of cardiomyocytes within the MSC tissue seemed to be rare. Thus, this improvement may be explained mainly by growth factor–mediated paracrine effects of the MSC sheet and a decrease in left ventricle wall stress resulting from the thick MSC tissue. Furthermore, no rats treated with the monolayered MSCs died during the study period, although untreated rats died frequently. These results indicate that fatal arrythmogenic problems were not caused by integration of the MSC tissue.

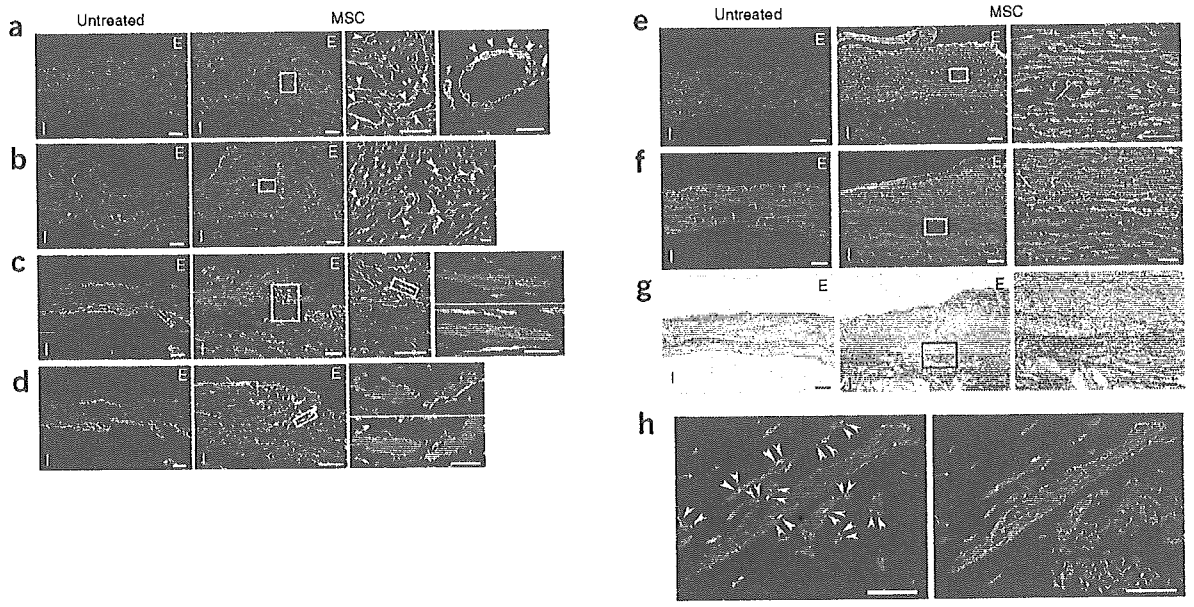

Figure 4 Differentiation of MSCs within the MSC tissue after growth *in situ*. (**a**,**b**) GFP-expressing MSCs (green) were identified as a thick stratum at the epicardial side of the myocardium. The MSC tissue contained a number of vascular structures positive for vWF (red, **a**) and αSMA (red, **b**). MSCs that did not participate in blood vessel formation were only rarely positive for αSMA, a marker for myofibroblasts. Arrows indicate transplanted MSCs positive for vWF or αSMA. (**c**,**d**) Some MSCs within the MSC tissue were positive for cardiac markers cardiac troponin T (red, **c**) and desmin (red, **d**). (**e**) Most of the MSC tissue was positive for vimentin (red). (**f**) The MSC tissue modestly stained for collagen type 1 (red). (**g**) Collagen deposition was also detected by picrosirius red staining. (**h**) FISH analysis. Newly formed cardiomyocytes that were positive for GFP (green) had only one set of X (purple) and Y chromosomes (white), whereas two X chromosomes were detected exclusively in GFP$^-$ host-derived cells. Nuclei are stained with DAPI (blue, **a**–**f** and **h**). Scale bars in left three panels of **a**–**g**, 100 μm; in **h** and far right panels of **a**–**g**, 20 μm. E, epicardial side; I, intimal side.

In summary, adipose tissue–derived monolayered MSCs can be readily engrafted to the scarred myocardium, grow gradually *in situ* and become a thick stratum that includes newly formed vessels, cardiomyocytes and undifferentiated MSCs. The engrafted MSCs reversed wall thinning in the scar area and improved cardiac function and survival in rats with myocardial infarction. Thus, transplantation of monolayered MSCs may be a new therapeutic strategy for cardiac tissue regeneration.

METHODS

Model of heart failure. All protocols were performed in accordance with the guidelines of the Animal Care Ethics Committee of the Japanese National Cardiovascular Center Research Institute. We used male Sprague-Dawley rats (Japan SLC) weighing 187–215 g. A myocardial infarction model was produced by ligation of the left coronary artery, as described previously[30]. Briefly, we anesthetized rats with sodium pentobarbital (30 mg/kg) and ventilated them with a volume-regulated respirator. We exposed hearts by left thoracotomy, and ligated the left coronary artery 2–3 mm from its origin between the pulmonary artery conus and the left atrium with a 6-0 Prolene suture. The sham group underwent thoracotomy and cardiac exposure without coronary ligation. The surviving rats were maintained on standard rat chow.

Study protocol. We randomly placed rats into four groups: rats with chronic heart failure that underwent transplantation of monolayered MSCs (MSC group; $n = 12$), rats with chronic heart failure given monolayered DFBs (DFB group; $n = 12$), rats with chronic heart failure without transplantation (untreated group; $n = 12$) and sham-operated rats without transplantation (sham group; $n = 10$). Four weeks after coronary ligation, the MSC and DFB groups underwent autologous transplantation of each monolayered cell graft onto the anterior wall, including the scar area (**Supplementary Methods** online). The other two groups underwent the same operative procedures without transplantation. We performed hemodynamic studies, echocardiography and histological assessments 4 and 8 weeks after coronary ligation (**Supplementary Methods**). Upon killing at 8 weeks after coronary ligation, only those rats with infarct size > 25% of the left ventricle area were included in this study. Therefore, the variation in infarct size between the experimental rats was relatively low (28–41%, average 33.9% ± 1.9%).

Isolation and culture of MSCs from adipose tissue. Immediately after coronary ligation, we acquired subcutaneous adipose tissue (1.1 ± 0.1 g) from the right inguinal region of each rat. We minced adipose tissue with scissors and digested it with 10 ml of type 1 collagenase solution (0.1 mg/ml, Worthington Biochemical) for 1 h in a 37 °C water bath shaker. After filtration with mesh filter (Costar 3480, Corning) and centrifugation at 780*g* for 8 min, we suspended isolated cells in α-MEM supplemented with 10% FCS and antibiotics, plated them onto a 100-mm dish and incubated them at 37 °C with 5% CO_2. A small number of spindle-shaped cells were apparent in visible symmetric colonies by days 5–7.

Preparation of temperature-responsive dishes. Specific procedures for preparation of square-designed PIPAAm-grafted dishes have been previously described[9]. Briefly, we spread IPAAm monomer (Kohjin) in 2-propanol solution onto 60-mm polystyrene culture dishes (Corning). We then subjected the dishes to irradiation (0.25-MGy electron beam dose) using an Area Beam Electron Processing system (Nisshin High-Voltage) to immobilize IPAAm on the dish surface; we then rinsed dishes with cold distilled water and dried them in nitrogen gas. In the second step, we masked the PIPAAm-grafted surface with a square glass coverslip (24 × 24 mm, Matsunami Glass). We spread acrylamide (AAm) monomer solution in 2-propanol onto the masked dish surface. We then irradiated the dish surface with an electron beam and washed it. As a result, the central square area of each dish was PIPAAm grafted (temperature responsive), and the surrounding border was poly-AAm grafted (non–cell adhesive). This PIPAAm-grafted surface is hydrophobic under culture

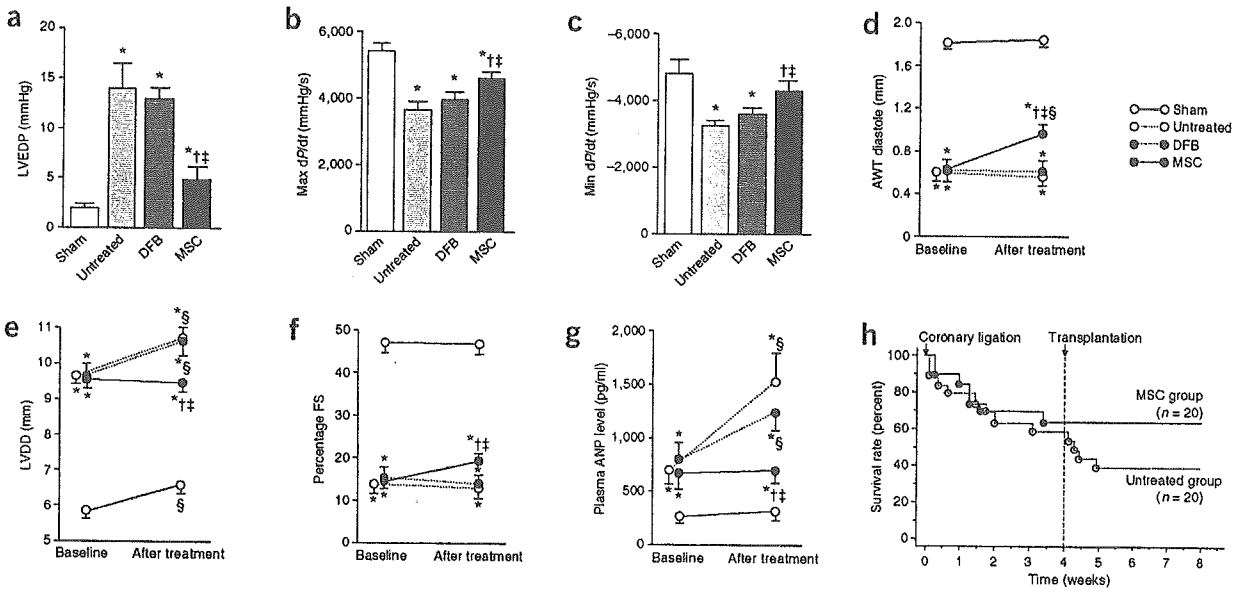

Figure 5 Cardiac structure and function after transplantation of monolayered MSCs. (**a–c**) Hemodynamic parameters obtained by catheterization. LVEDP, left ventricle end-diastolic pressure. (**d–f**) Echocardiographic findings. AWT, anterior wall thickness; LVDD, left ventricle end-diastolic dimension; FS, fractional shortening. (**g**) Plasma atrial natriuretic peptide (ANP) level. Baseline represents measurements 4 weeks after coronary ligation; 'after treatment' represents measurements taken 4 weeks after transplantation (8 weeks after coronary ligation). Data are mean ± s.e.m. $^{*}P < 0.05$ versus sham group; $^{\dagger}P < 0.05$ versus untreated group; $^{\ddagger}P < 0.05$ versus DFB group; $^{\S}P < 0.05$ versus baseline. (**h**) Survival of rats with chronic heart failure with or without monolayered MSC transplantation. The Kaplan-Meier survival curve demonstrates an 8-week survival rate of 65% for the MSC group versus 45% for the untreated group. Survival rate after transplantation was significantly higher in the MSC group than in the untreated group (100% versus 71% 4-week survival rate after transplantation, log-rank test, $P < 0.05$).

conditions at 37 °C and becomes reversibly hydrophilic below 32 °C. Therefore, cultured cells that adhere to the dish surface spontaneously detach from the grafted surface without enzymatic digestion.

Preparation of monolayered cell grafts. We suspended MSCs at the third or fourth passage from adipose tissue or DFBs at the second passage by trypsinization, and plated the cell suspension containing 3 ml of complete medium onto a 60-mm temperature-responsive dish at 5×10^5 cells per dish (MSCs) or 8×10^5 cells per dish (DFBs) and cultured cells at 37 °C. After 3 d of culture, confluently cultured MSCs or DFBs on the temperature-responsive dishes were incubated at 20 °C. By 40 min, both MSCs and DFBs detached spontaneously and floated up into the medium as monolayered cell grafts. Immediately after detachment, we gently aspirated the monolayered cell grafts using a 1,000 µl pipette tip and transferred them onto an elastic plastic sheet.

Statistical analysis. Numerical values are expressed as mean ± s.e.m. There are four groups of continuous variables in this study. Therefore, for multiple comparisons of more than two groups, we performed one-way analysis of variance (ANOVA). If the ANOVA was significant, we used the Newman-Keul procedure as a *post hoc* test. For repeated measurement such as echocardiographic parameters, we performed two-way repeated ANOVA with the Newman-Keul test. Comparisons of parameters between two groups were made by unpaired Student *t*-test. A value of $P < 0.05$ was considered significant.

Note: Supplementary information is available on the Nature Medicine website.

ACKNOWLEDGMENTS

We thank J.I. Hoffman for his statistical advice. We thank T. Iwase, T. Ito, S. Murakami, N. Sakata and Y. Isono for their technical support. We thank Y. Tsuboi and H. Sonoda for their assistance with microscopic analysis of monolayered cell grafts. We also thank Y. Sawa for his suggestions on this study. This work was supported by research grants for Cardiovascular Disease (16C-6) and Human Genome Tissue Engineering 005 and 009 from the Japanese Ministry of Health, Labor and Welfare, and the Program for Promotion of Fundamental Studies in Health Science of the Japanese National Institute of Biomedical Innovation.

COMPETING INTERESTS STATEMENT

The authors declare competing financial interests (see the *Nature Medicine* website for details).

Published online at http://www.nature.com/naturemedicine/
Reprints and permissions information is available online at http://npg.nature.com/reprintsandpermissions/

1. Liu, J. *et al.* Autologous stem cell transplantation for myocardial repair. *Am. J. Physiol. Heart Circ. Physiol.* **287**, H501–H511 (2004).
2. Reinlib, L. & Field, L. Cell transplantation as future therapy for cardiovascular disease?: A workshop of the National Heart, Lung, and Blood Institute. *Circulation* **101**, E182–E187 (2000).
3. Schuster, M.D. *et al.* Myocardial neovascularization by bone marrow angioblasts results in cardiomyocyte regeneration. *Am. J. Physiol. Heart Circ. Physiol.* **287**, H525–H532 (2004).
4. Kocher, A.A. *et al.* Neovascularization of ischemic myocardium by human bone-marrow-derived angioblasts prevents cardiomyocyte apoptosis, reduces remodeling and improves cardiac function. *Nat. Med.* **7**, 430–436 (2001).
5. Bel, A. *et al.* Transplantation of autologous fresh bone marrow into infarcted myocardium: a word of caution. *Circulation* **108**, II247–II252 (2003).
6. Yamada, N. *et al.* Thermo-responsive polymeric surface: control of attachment and detachment of cultured cells. *Makromol. Chem. Rapid Commun.* **11**, 571–576 (1990).
7. Okano, T., Yamada, H., Sakai, H. & Sakurai, Y. A novel recovery system for cultured cells using plasma-treated polystyrene dishes grafted with poly (N-isopropylacrylamide). *J. Biomed. Mater. Res.* **27**, 1243–1251 (1993).
8. Shimizu, T. *et al.* Fabrication of pulsatile cardiac tissue grafts using a novel 3-dimensional cell sheet manipulation technique and temperature-responsive cell culture surfaces. *Circ. Res.* **90**, e40–e48 (2002).
9. Hirose, M., Kwon, O.H., Yamato, M., Kikuchi, A. & Okano, T. Creation of designed shape cell sheets that are noninvasively harvested and moved onto another surface. *Biomacromolecules* **1**, 377–381 (2000).
10. Kushida, A. *et al.* Decrease in culture temperature releases monolayer endothelial cell sheets together with deposited fibronectin matrix from temperature-responsive culture surfaces. *J. Biomed. Mater. Res.* **45**, 355–362 (1999).
11. Herreros, J. *et al.* Autologous intramyocardial injection of cultured skeletal muscle-derived stem cells in patients with non-acute myocardial infarction. *Eur. Heart J.* **24**, 2012–2020 (2003).

12. Skobel, E. *et al.* Transplantation of fetal cardiomyocytes into infarcted rat hearts results in long-term functional improvement. *Tissue Eng.* **10**, 849–864 (2004).
13. Hodgson, D.M. *et al.* Stable benefit of embryonic stem cell therapy in myocardial infarction. *Am. J. Physiol. Heart Circ. Physiol.* **287**, H471–H479 (2004).
14. Makino, S. *et al.* Cardiomyocytes can be generated from marrow stromal cells in vitro. *J. Clin. Invest.* **103**, 697–705 (1999).
15. Pittenger, M.F. *et al.* Multilineage potential of adult human mesenchymal stem cells. *Science* **284**, 143–147 (1999).
16. Reyes, M. *et al.* Origin of endothelial progenitors in human postnatal bone marrow. *J. Clin. Invest.* **109**, 337–346 (2002).
17. Toma, C., Pittenger, M.F., Cahill, K.S., Byrne, B.J. & Kessler, P.D. Human mesenchymal stem cells differentiate to a cardiomyocyte phenotype in the adult murine heart. *Circulation* **105**, 93–98 (2002).
18. Wang, J.S. *et al.* Marrow stromal cells for cellular cardiomyoplasty: feasibility and potential clinical advantages. *J. Thorac. Cardiovasc. Surg.* **120**, 999–1005 (2000).
19. Jiang, Y. *et al.* Pluripotency of mesenchymal stem cells derived from adult marrow. *Nature* **418**, 41–49 (2002).
20. Nagaya, N. *et al.* Transplantation of mesenchymal stem cells improves cardiac function in a rat model of dilated cardiomyopathy. *Circulation* **112**, 1128–1135 (2005).
21. Rangappa, S., Fen, C., Lee, E.H., Bongso, A. & Wei, E.S. Transformation of adult mesenchymal stem cells isolated from the fatty tissue into cardiomyocytes. *Ann. Thorac. Surg.* **75**, 775–779 (2003).
22. Zuk, P.A. *et al.* Human adipose tissue is a source of multipotent stem cells. *Mol. Biol. Cell* **13**, 4279–4295 (2002).
23. Gaustad, K.G., Boquest, A.C., Anderson, B.E., Gerdes, A.M. & Collas, P. Differentiation of human adipose tissue stem cells using extracts of rat cardiomyocytes. *Biochem. Biophys. Res. Commun.* **314**, 420–427 (2004).
24. Planat-Benard, V. *et al.* Plasticity of human adipose lineage cells toward endothelial cells: physiological and therapeutic perspectives. *Circulation* **109**, 656–663 (2004).
25. Lee, R.H. *et al.* Characterization and expression analysis of mesenchymal stem cells from human bone marrow and adipose tissue. *Cell. Physiol. Biochem.* **14**, 311–324 (2004).
26. Li, J., Takaishi, K., Cook, W., McCorkle, S.K. & Unger, R.H. Insig-1 "brakes" lipogenesis in adipocytes and inhibits differentiation of preadipocytes. *Proc. Natl. Acad. Sci. USA* **100**, 9476–9481 (2003).
27. Vande Berg, J.S., Rudolph, R. & Woodward, M. Comparative growth dynamics and morphology between cultured myofibroblasts from granulating wounds and dermal fibroblasts. *Am. J. Pathol.* **114**, 187–200 (1984).
28. Nishida, K. *et al.* Corneal reconstruction with tissue-engineered cell sheets composed of autologous oral mucosal epithelium. *N. Engl. J. Med.* **351**, 1187–1196 (2004).
29. Shimizu, T., Yamato, M., Kikuchi, A. & Okano, T. Cell sheet engineering for myocardial tissue reconstruction. *Biomaterials* **24**, 2309–2316 (2003).
30. Nishikimi, T., Uchino, K. & Frohlich, E.D. Effects of α1-adrenergic blockade on intrarenal hemodynamics in heart failure rats. *Am. J. Physiol. Regul. Integr. Comp. Physiol.* **262**, R198–R203 (1998).

A Novel Micro-Angiography Detecting Angiogenesis, Application for Autologous Bone Marrow Mononuclear Cells Transplantation in the Patients with Critical Limb Ischemia

Kazuhiro Nishigami, Takeshi Nakatani, Masaaki Chiku, Hidezo Mori

National Cardiovascular Center, 5-7-1 Fujishiro-dai, Suita, Osaka 565-8565, Japan

Summary. Conventional Anigiographic Findings in Autologous Bone Marrow Mononuclear Cells Transplantation for Critical Limb Ischemia: Bone marrow mononuclear cells have many of the characteristics of stem cells for mesenchymal tissues, and secrete many angiogenic cytokines. We performed autologous transplantation of bone marrow mononuclear cells in six patients with critical limb ischemia due to Buerger disease, who were not candidates for catheter or surgical revascularization. Leg pains at rest and skin ulcers improved after bone marrow transplantation in all patients, although significant collateral developments after the therapy by conventional angiography could not be observed. Autologous transplantation of bone marrow mononuclear cells including stem cells improved critical limb ischemia due to Buerger disease. Neovascularization after therapeutic angiogenesis might be quite small and could not be visualized by conventional angiography.

Novel Micro-angiograpy:We developed in-hospital micro-angiographic equipment which consisted of a high power X-ray source for computed tomography and an avalanche type detector characterized by a high spatial resolution (20μm) and high sensitivity (100 times of CCD camera). We visualized mid-zone collaterals after femoral arterial exfoliation with and without therapeutic angiogenesis in rabbit ischemic limbs and assessed the radio-absorptions in a clinical setting. The micro-angiography clearly demonstrated mid-zone collaterals after the treatment with a diameter of down to 50μm, but the conventional angiography did not. The sum of ra-

dio-absorptions for 10 seconds in clinical settings was 300 mSv. The newly developed in-house micro-angiography could illuminate micro-vessels with a diameter of down to 50μm in clinical settings safely and could be useful in the evaluation of therapeutic angiogenesis.

Keywords. Micro-angiography, Angiogenesis, Autologous bone marrow mononuclear cells transplantation, Critical limb ischemia, Buerger disease

Introduction

Endothelial progenitor cells (EPCs) possess the ability to mature into cells that line the lumen of blood vessels(Asahara T, et al. 1997). Therapeutic angiogenesis could be induced by the transplantation of bone marrow mononuclear cells including EPCs. Several studies demonstrated that therapeutic angiogenesis using autologous bone marrow mononuclear cells transplantation (BMT) was effective for ischemic vascular diseases although conventional angiography could not precisely detect developed collaterals after therapeutic angiogenesis(Iba O, et al. 2002, Inaba S, et al. 2002, Shintani S, et al. 2001,Tateishi-Yuyama E, et al. 2002). We developed an in-hospital micro-angiographic equipment which consisted of a high power X-ray source for computed tomography and an avalanche type detector characterized by a high spatial resolution (20μm) and high sensitivity (100 times of CCD camera).

The purpose of the present study was to evaluate the clinical effects and conventional angiographic findings on BMT for critical limb ischemia, and to validate the usefulness and safety of the novel micro-angiography technique for the evaluation of therapeutic angiogenesis.

Methods

Patients

Patients qualified for autologous BMT if they had chronic critical limb ischemia including rest pain and/or non-healing ischemic ulcers for a minimum of 4 weeks without evidence of improvement in response to

conventional therapies and were not optimal candidates for surgical or catheter revascularization. Buerger's disease was diagnosed by segmental occlusion of small- and medium-sized arteries, absence of atherosclerosis, and corkscrew collaterals circumventing the occlusion in angiogram and the exclusion of autoimmune diseases such as scleroderma or systemic lupus erythematosus, hypercoagulable states, diabetes, or acute arterial occlusion secondary to embolism. Patients with retinopathy and/or malignancy were excluded. Although 30 patients with atherosclerotic peripheral artery disease were candidates for BMT, they were excluded from the present study due to their systemic atherosclerotic complications. Six patients with Buerger's disease were recruited for the present study. All patients had legs pain at rest and five patients had foot ulcers. Written consent was obtained from all participants of this study. This clinical trial of autologous BMT for the treatment of patients with critical ischemia was approved by the Medical Ethics Committee of the National Cardiovascular Center.

Autologous BMT

Bone marrow fluid (700-800ml) was collected from the iliac bone under general anesthesia. The harvested bone marrow fluid was diluted with RPMI 1640 (Nikken Bio Medical Laboratory, Kyoto, Japan) containing heparin, then stored in a sterile pack from the Bone Marrow Collection Kit (Baxter, IL, USA). The mononuclear cell fraction was prepared with a Fresenius AS104 (AMCO, USA). The injection volume was 0.5ml and injections were spaced 2-3cm apart, using a 1ml syringe and a 27-gauge needle. Leg pains were measured by a visual analog pain scale and foot ulcers were evaluated by area and appearance.

Novel micro-angiography

The in-hospital micro-angiographic equipment consisted of a high power X-ray source for computed tomography and an avalanche type detector characterized by a high spatial resolution (20μm) and high sensitivity (100 times of CCD camera) (Fig.1).

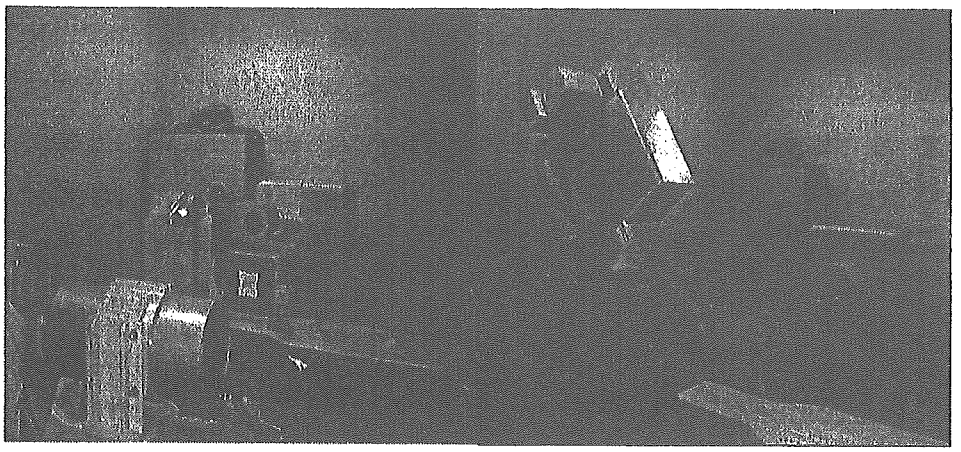

a b

Fig. 1a, b. The micro-angiographic equipment that we developed. High-voltage power X-ray source a and a detecting system with a high spatial resolution(25μm) and high sensitivity (100 times of CCD camera) b.

Limb ischemia models in rabbits were made by ligating the femoral artery and treated by fibroblast growth factor 4 (FGF-4) genes incorporated to gelatin hydro gel (GHG). One month after the treatment, we evaluated collateral micro-vessels by using conventional and micro-angiographic systems. The approach was via the left femoral artery so that the catheter was located in the abdominal aorta. A 5ml bolus of Iodine contrast medium (300mg/ml) was injected at 3ml/sec using an auto-injection system. Imaging was recorded using a digital source in 1000 x 1000 pixels. The sum of radio-absorptions for 10 seconds in clinical settings was studied.

Results

Autologous BMT for Critical Limb Ischemia

The number of transplanted bone marrow mononuclear cells were one to five multiplied 10^9. Rest pains decreased or disappeared in one month after BMT (Fig.2) and Skin ulcers improved in one to three months after BMT in all patients (Fig.3).